Molecular-dynamics studies on defect-formation processes during crystal growth of silicon from melt

Manabu Ishimaru, Shinji Munetoh, and Teruaki Motooka
Department of Materials Science and Engineering, Kyushu University, Hakozaki, Fukuoka 812-8581, Japan

Koji Moriguchi and Akira Shintani
Advanced Technology Research Laboratories, Sumitomo Metal Industries, Ltd., Amagasaki, Hyogo 660, Japan
(Received 6 April 1998; revised manuscript received 1 June 1998)

We have performed molecular-dynamics calculations to examine defect-formation processes in silicon grown from the melt based on the ordinary Langevin equation employing the Tersoff interatomic potential. Our simulations indicated that hexagonal structures are formed near the solid-liquid interfaces and these regions give rise to microfacets composed of primarily {111} planes. Most of these hexagonal configurations were annihilated during further crystal growth, but a part of them were left, which resulted in defect formation with five- and seven-member rings. [S0163-1829(98)09943-3]

Reduction of defects in crystal silicon (c-Si) wafers is strongly required as device sizes are decreased in Si integrated circuits. These c-Si wafers are mostly produced from the liquid phase by using the pulling (Czochralski) or floating-zone methods, and it is known that defect formation in the obtained crystals strongly depends on the growth conditions such as crystal growth rates and temperature gradients at the c-Si and liquid Si (l-Si) interfaces. Therefore, understanding the defect-formation mechanisms from l-Si is of technological importance to reduce defects in c-Si. However, microscopic structures of the defects as well as their formation mechanisms are not well understood, because high melting temperature and intensive reactivity of l-Si have inhibited extensive experimental studies.

The molecular-dynamics (MD) calculation is a powerful tool for studying dynamical processes of crystal growth, and many researchers[1–6] have performed MD simulations of solidification from melted Si. Based on an empirical interatomic potential for Si proposed by Stillinger and Weber,[7] Landman and co-workers[1–3] simulated the liquid-phase epitaxial growth onto Si substrates, by extracting heat from the system (~1000 atoms) through two crystal layers at the boundary of the MD cell. They found the appearance of lattice defects near the solid-melt interface during crystal growth in the [111] direction, but these defects were eliminated due to *dynamical self-annealing*; accordingly defect-free c-Si was obtained. In addition, as far as we know, no investigations have been conducted for the defect-formation processes during crystal growth in the [001] direction, which is the most popular pulling direction in production of c-Si wafers.

We[8–10] have recently performed MD simulations using the Tersoff interatomic potential[11] in order to reveal the atomistic structures of l-Si and the crystallization mechanisms from l-Si, and have shown that the Tersoff potential is useful to reproduce experimental results. In the present study, we carried out MD simulations of the crystal growth on the (001) faces and examined the structures of defects and their formation processes.

The 9216 Si atoms were at first placed on the diamond lattice sites in the MD cell with a constant volume of $62.0\times62.0\times42.0$ Å^3 (tetragonal prism), which gives the density of l-Si, 2.58 g/cm^3. Periodic boundary conditions were employed in the [100] and [010] directions. This MD cell was immersed in a heat bath with the fixed temperature distribution and pulled in the [001] direction for the simulation of the crystal growth on the (001) faces. The pulling speed and temperature gradient were set to be 12 m/s and 15 K/Å, respectively. In the [001] or Z direction, the atomic positions in the top two layers (the lower-temperature side) were fixed, while the bottom (the higher-temperature side) was assumed to be a free surface. A reflection wall was set at 2 Å away from the bottom layer to prevent atoms from escaping from the MD cells. The temperature gradient was controlled by the Langevin equation

$$m\ddot{\mathbf{r}}_i(t) = -\gamma\dot{\mathbf{r}}_i(t) + \mathbf{F}_i + \mathbf{R}_i\{t, Z_i(t)\},$$

where m is the atomic mass, $\mathbf{r}_i(t)$ the position vector of the ith atom at time t, $\mathbf{F}_i(t)$ is the interatomic force calculated by the Tersoff potential, γ is the friction constant, $\mathbf{R}_i\{t, Z_i(t)\}$ is the random force, and $Z_i(t)$ is the Z coordinates of atoms. We employed the scheme developed by van Gusteren and Berendsen[12] for numerical integration of Langevin equations using a time step of 2×10^{-3} ps and a friction constant of $5.0\ \mathrm{ps}^{-1}$.

Figure 1 shows the atomic arrangements in (a) the initial stage of the crystallization process, (b) after 267 ps, and (c) after 533 ps. These figures were obtained by projecting the all atomic positions in selected regions of the MD cells on the $(\bar{1}10)$ plane. The initial state was made by heating c-Si for 600 ps in the thermal bath with the temperature distribution as shown in Fig. 1(a), and the system was found to reach the steady state during this period as judged by the total energies. The crystal-melt interface is rough and located between 2300 and 2400 K in Fig. 1(a), and the interface was confirmed to fluctuate spatially and temporally. This temperature is higher than the melting temperature of Si (1687 K), since the Tersoff potential is not adjusted to fit any

 ©1998 The American Physical Society

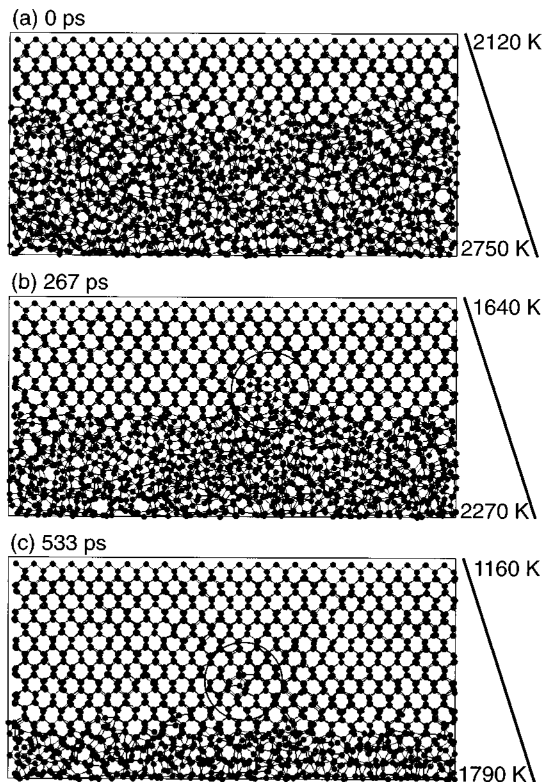

FIG. 1. Three snapshots taken during the [001] pulling: (a) initial stage of the crystallization process, (b) after 267 ps, and (c) after 533 ps. The time shown in these diagrams represents that after equilibration. All atomic positions are projected on the $(\bar{1}10)$ plane. Solid lines of the right-hand sides denote temperature distributions at each stage of the crystallization.

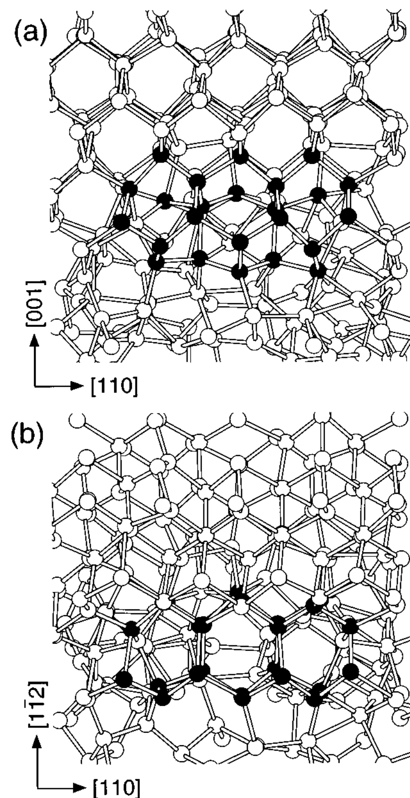

FIG. 2. Atomic arrangements near the crystal-melt interface encircled in Fig. 1(b). (a) $[\bar{1}10]$ and (b) $[\bar{1}11]$ views. A bond is drawn if its distance is within a cutoff of 2.90 Å.

liquid-phase data. However, high melting temperature itself is not an essential problem in the present study, because our purpose is to examine the defect-formation processes and solid-melt interfacial structures during the crystal growth from melted Si. The Tersoff liquid, which possesses the same structures as real l-Si,[8,9] is cooled from just above the melting temperature of the potential, thus the situation is considered to be similar to that of experiments.

As the pulling time increases, the locations of the interface move downward and the crystallization occurs. In Fig. 1(b), the solid-liquid interface exists around ~2000 K and l-Si is supercooled. It should be noted that the crystallized region enclosed in Fig. 1(b) includes the atomic configuration, which is different from that of (001)Si. This region possesses a different structure from that of the surrounding c-Si region and causes microfacets composed of primarily {111} planes. Most of the misoriented configurations are annihilated during the further growth due to back melting or *dynamical self-annealing* as pointed out by Luedtke *et al.*[3] In Fig. 1(c), l-Si transforms into glass for rapid quenching rates and the crystallization can no longer occur. In previous MD simulations using ~1000 Si atoms,[1–3] no isolated defects were created in c-Si. In the present study, on the other hand, we succeeded in generating an ''elementary'' grown-in defect for the first time by using large-scale MD calculations (~10 000 Si) [Fig. 1(c)]. This defect is due to the misoriented configurations described above.

To obtain more detailed structures of the crystal-liquid interfaces and the defect, magnified pictures of the regions encircled in Fig. 1 are given in Figs. 2 and 3. In Figs. 2(a) and 2(b), the atomic configurations are projected on the $(\bar{1}10)$ and $(\bar{1}11)$ planes, respectively. In addition to the c-Si region with the [001] orientation, different configurations marked by black circles exist near the solid-liquid interface. These arrangements in Figs. 2(a) and 2(b) correspond to the hexagonal structure observed in the $[\bar{1}011]$ and [0001] directions, respectively; accordingly the hexagonal Si is grown epitaxially on the cubic Si. This hexagonal structure is locally stable, because the nearest-neighbor structure of hexagonal Si is the same as that of cubic Si. Therefore, these regions disturb further (001) crystallization and induce prominent {111} microfacets as seen in Fig. 1(b). Similar microstructures were also observed in MD simulations of growth of microcrystals embedded in an amorphous Si matrix,[13] but the crystal orientation relationship between the hexagonal and cubic Si is different from that in the present case.

It should be noted that the obtained defect is not the single vacancy that is considered as an elementary defect in c-Si. It can be seen that several atoms shift from the single c-Si sites and five- and seven-member rings exist in Fig. 3(a). The bond lengths and angles between the first nearest neighbors around the defects were confirmed to be almost equal to those of c-Si, thus the tetrahedral structure is still maintained around each atom. However, the atomic arrangement marked by black circles is different from that of c-Si; i.e., their stacking sequence possesses the eclipse configuration. The structure of the obtained ''elementary'' grown-in defect is similar to that generated by the divacancy and di-interstitial

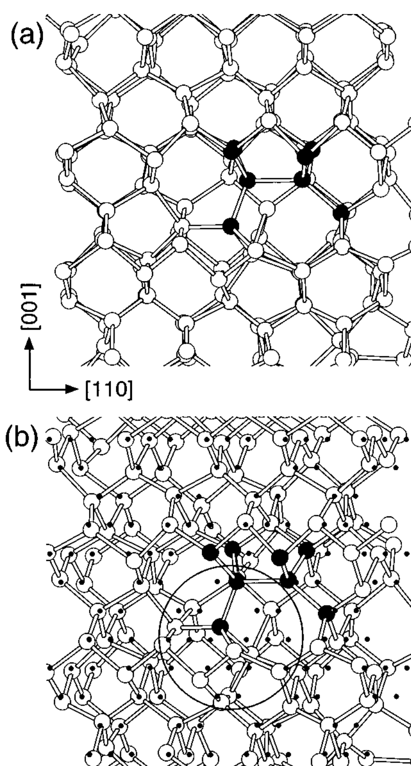

FIG. 3. Magnified pictures around the defects encircled in Fig. 1(c). (a) [110] view and (b) 15° inclined in the [$\bar{1}$10] direction around the [001] axis. The perfect c-Si structure denoted by black points is superimposed in (b).

pair model proposed previously.[14] Our present result is consistent with the fact that electron-spin-resonance signals of single vacancy have never been observed in Czochralski-grown c-Si wafers.

To determine the defect nature, a tilted picture of Fig. 3(a) is exhibited in Fig 3(b). The black points indicate the lattice sites of perfect c-Si. The 19 lattice sites (black points) are contained in the region encircled in Fig. 3(b), while there exist only 16 Si atoms (open circles) in the same region. (One black point is superimposed on the black circle.) That is, three Si atoms are missing around the ''elementary'' grown-in defect. The missing Si atoms did not exist in the crystallized region as the interstitial atoms, thus they should have diffused into melted Si. These defects may well be transformed into c-Si with a microvoid when they combine with each other, because the number of the Si atoms is smaller than that of the lattice sites of perfect c-Si. This microvoid becomes the cause of vacancy-type defects such as the crystal originated particle, flow pattern defect, and laser scattering tomography defect, which are observed experimentally in Czochralski-grown c-Si ingots. Our present simulations explain a possible formation process of the vacancy-type defects (void), while the interstitial-type defects also exist in real c-Si. The kind of the grown-in defects has been pointed out to depend strongly on the pulling speeds and temperature gradients during the crystal growth;[15] therefore it is important to clarify the effects of these growth parameters on the defect formation and the quality of c-Si. More extensive study is currently underway.

It is important to relate the MD results with macroscopic growth rates and temperature gradients. Thus, further investigation should be necessary to develop a scaling theory such as a renormalization-group theory in which the scaling property of the ensemble average of the relevant physical quantity can be obtained based on microscopic equations. However, the main purpose of the present paper is not to examine the effects of the temperature gradients and growth speed on crystal growth but to obtain a microscopic picture of defect-formation processes. Since the size and time are limited in MD simulations, it is inevitable to use unrealistic growth conditions such as crystal growth rates and temperature gradients. Nevertheless, the obtained result gives a possible defect-formation process during crystal growth of Si from the melt. We think this is one of the basic advantages of MD simulations.

In summary, we have shown a microscopic picture for defect formation mechanisms during the (001) pulling from melted Si. It was found that the epitaxially grown hexagonal structures appear near the solid-liquid interfaces and become the cause of microfacets established on the {111} planes. These misoriented configurations mostly disappeared during the further crystallization, but a part of them remained and isolated defects were formed in c-Si. Our MD simulations suggested that the ''elementary'' grown-in defects of c-Si generated from the melt are not the point defects such as single vacancy but they consist of the odd-member rings, which resemble a defect structure formed by a combination of the divacancy and di-interstitial pair.

This work was conducted as JSPS Research for the Future Program in the Area of Atomic-Scale Surface and Interface Dynamics under the project of ''Dynamic Behavior of Silicon Atoms, Lattice Defects and Impurities near Silicon Melt-crystal Interface.'' We would like to thank T. Kumamoto and K. Yoshida for their assistance on molecular-dynamics calculations. Part of this work is the result of ''Technology for Production of High Quality Crystal,'' which is supported by the New Energy and Industrial Technology Development Organization through the Japan Space Utilization Promotion Center in the program of the Ministry of International Trade and Industry. M.I. acknowledges partial support from the Sumitomo Foundation and Iketani Science and Technology Foundation.

[1] U. Landman, W. D. Luedtke, R. N. Barnett, C. L. Cleveland, M. W. Ribarsky, E. Arnold, S. Ramesh, H. Baumgart, A. Martinez, and B. Khan, Phys. Rev. Lett. **56**, 155 (1986).

[2] U. Landman, W. D. Luedtke, M. W. Ribarsky, R. N. Barnett, and C. L. Cleveland, Phys. Rev. B **37**, 4637 (1988).

[3] W. D. Luedtke, U. Landman, M. W. Ribarsky, R. N. Barnett, and C. L. Cleveland, Phys. Rev. B **37**, 4647 (1988).

[4] J. Q. Broughton and F. F. Abraham, J. Cryst. Growth **75**, 613 (1986).

[5] M. D. Kluge and J. R. Ray, Phys. Rev. B **39**, 1738 (1989).

[6] F. X. Kelly and L. H. Unger, J. Cryst. Growth **102**, 658 (1990).

[7] F. H. Stillinger and T. A. Weber, Phys. Rev. B **31**, 5262 (1985).

[8] M. Ishimaru, K. Yoshida, and T. Motooka, Phys. Rev. B **53**, 7176 (1996).
[9] M. Ishimaru, K. Yoshida, T. Kumamoto, and T. Motooka, Phys. Rev. B **54**, 4638 (1996).
[10] M. Ishimaru, S. Munetoh, and T. Motooka, Phys. Rev. B **56**, 15 133 (1997).
[11] J. Tersoff, Phys. Rev. B **38**, 9902 (1988).
[12] W. F. van Gunsteren and H. J. C. Berendsen, Mol. Phys. **45**, 637 (1982).
[13] L. A. Marqués, M.-J. Caturla, T. Díaz de la Rubia, and G. H. Gilmer, J. Appl. Phys. **80**, 6160 (1996).
[14] T. Motooka, Phys. Rev. B **49**, 16 367 (1994).
[15] W. V. Ammon, E. Dornberger, H. Oerkrug, and H. Weidner, J. Cryst. Growth **151**, 273 (1995).